This article has been accepted for publication in a future issue of this journal, but has not been fully edited. Content may change prior to final publication. Citation information: DOI 10.1109/TIE.2014.2331011, IEEE Transactions on Industrial Electronics

Soft-Switching AC-Link Three-Phase AC-AC Buck-Boost Converter

Mahshid Amirabadi, *Member, IEEE*, Jeihoon Baek, *Member, IEEE*, Hamid A. Toliyat, *Fellow, IEEE* and William C. Alexander, *Member, IEEE*

***Abstract*— In this paper, the soft-switching ac-link ac-ac buck-boost converter will be studied in more detail. This single-stage converter, which is in essence an extension of the dc-dc buck-boost converter, can be an excellent alternative to dc-link converters. Being a buck-boost converter, this converter is capable of both stepping-up and stepping-down the voltage. The link current and voltage are both alternating and their frequency can be as high as permitted by the switches and the sampling time of the microcontroller. This eliminates the need for dc inductors or dc electrolytic capacitors, and the main energy storage element is an ac inductor (L). Moreover, in this converter galvanic isolation can be provided by adding a single-phase high frequency transformer to the link. Therefore, the proposed converter is expected to be more compact compared to the conventional dc-link converter. The [illegible] effect of the LC link resonance on the performance of the converter will be studied. This analysis helps evaluating the performance of the converter at low power levels when the resonating time of the LC link is not negligible. Using this analysis, the link peak current and the link frequency may be calculated at any point of operation. The accuracy of this method is verified through simulations and experiments. Detailed comparison of the proposed converter with the dc-link converter will be also presented in this paper. It will be shown that despite having more switches, the current rating of the switches is lower in this converter. Moreover, the efficiency of the two converters will be compared. Finally, the performance of the soft switching ac-link ac-ac buck-boost converter is experimentally evaluated in this paper. It will be shown that the converter has the possibility of both changing the frequency and the voltage. Both step-up and step-down operations will be verified through experiments.**

***Index Terms*—Soft-switching, ac-ac converter, buck-boost converter, ac link, high frequency ac link, zero voltage turn on, galvanic isolation, high frequency ac transformer**

I. Introduction

Three-phase ac-ac converters are needed in a variety of applications, including wind power generation and variable speed drives. Different types of ac-ac converters have been proposed over the years. These converters can be classified as direct or indirect depending on their power conversion type. Matrix converters and cycloconverters are examples of the direct ac-ac converters; whereas the dc-link and the ac-link converters are classified as indirect ac-ac converters [1-4]. Cycloconverters and matrix converters have several limitations that hinder their widespread use in industry. Among these limitations are the poor input displacement, low input power factor, and limited output frequency in the cycloconverters, and

boost rectifier and a three-phase buck inverter. Regardless of the type of the rectifier or the inverter, dc electrolytic capacitors are integral part of these converters. Electrolytic capacitors are very sensitive to temperature, and can cause severe reliability problems at higher temperatures. Therefore, converters that contain dc electrolytic capacitors have higher failure rates and shorter lifetimes compared to the other converters [5-7]. This is not the only problem with dc-link converters. In these converters galvanic isolation can be provided by three-phase low frequency transformers. Therefore, another limitation of the dc-link converters is the large size and the heavy weight of the low frequency transformers employed.

Resonant ac-ac converters, which are classified as ac-link converters, have been proposed as an alternative to dc-link converters [8]. In [9], the parallel ac voltage resonant converter was proposed. The link in this converter is formed by a parallel LC pair resonating continuously. Therefore, the passive link components need to have high reactive ratings and there is high power dissipation in the link. Moreover, the load inductance and capacitance can affect the link resonance. Hence, this type of converter is not suitable for all types of loads.

Despite the superficial resemblance between the parallel ac voltage link converter proposed in [8, 9] and the proposed configuration here, the principles of the operation of the two converters are totally different. In [8, 9] the link is resonating all the time; whereas in the proposed converter the link resonates just for a short portion of time in each cycle.

Manuscript received July 26, 2013; revised October 8, 2013, January 1, 2014 and March 24, 2014; accepted April 23, 2014.

M. Amirabadi is with University of Illinois at Chicago, IL 60607 USA, J. Baek is with Korea Railroad Research Institute, Uiwang, Korea, H.A. Toliyat is with Texas A&M University, College Station, TX 77843 USA, and W. C. Alexander is with Ideal Power Converters Inc., Spicewood, TX 78669 USA.

This article has been accepted for publication in a future issue of this journal, but has not been fully edited. Content may change prior to final publication. Citation information: DOI 10.1109/TIE.2014.2331011, IEEE Transactions on Industrial Electronics

Therefore, in [8, 9] both the link capacitor and the link inductor are required to allow the converter to operate properly; while in the proposed configuration the link capacitor may be removed and the converter can still operate. Apparently, no soft switching is offered when the capacitor is removed. The link current and voltage in [8, 9] are both sinusoidal, because the link resonates continuously. However, in the proposed configuration the link current is triangular and the link voltage is close to a square wave. In the parallel ac voltage link converter proposed in [8, 9], the terminals need to appear as current sources; therefore, inductors are placed at the terminals. However, in the proposed converter, similar to a buck-boost converter, we need voltage sources across the terminals.

Other than the above mentioned configurations, several other three-phase ac-ac topologies have been proposed. Two of them, which have led to the proposed configuration and are both classified as dc-link converters, are studied here. A hard-switching ac-ac buck-boost converter was proposed in [10]. This converter was an extension of the dc-dc buck-boost converter and was formed by twelve unidirectional switches. The link inductor current in this converter was dc and the switches had hard switching.

A partial resonant topology with twelve unidirectional switches was proposed in [11]. This converter was a soft-switching dc-link ac-ac buck-boost converter. Despite the high frequency of the link and the soft switching, this converter suffers from reduced utilization of the inductor due to the dc component of the link current, and also long quiescent resonant swing back time during which no power is transferred.

In this paper, a soft-switching ac-link ac-ac buck-boost converter, is introduced, studied, analyzed and evaluated. In this converter, the link current and voltage are both alternating and their frequency can be very high. This eliminates the need for the dc electrolytic capacitors and the low frequency transformers. In case galvanic isolation is required, a single-phase high-frequency transformer may be added to the link. The alternating link current and the short resonating modes of this converter solve the problems associated with the converter proposed in [11]. This topology was originally proposed in [12] and the present authors of this paper studied the principles of the operation and different applications of this converter in [13-21]. In [18] and [19] the application of this converter in photovoltaic power generation was studied and the performance of the dc to ac and hybrid dc to ac configurations were experimentally evaluated. This paper, on the other hand, focuses on the design and analysis of the three-phase ac-ac configuration, especially the effect of the resonance on the performance of the converter at low power levels. Although the analysis of this converter was studied in [17], the proposed procedure was not experimentally verified. This paper evaluates the performance of the ac-ac converter through both simulations and experiments. The detailed experimental results corresponding to the ac-ac configuration are presented in this paper. As will be shown, an important feature of this ac-ac

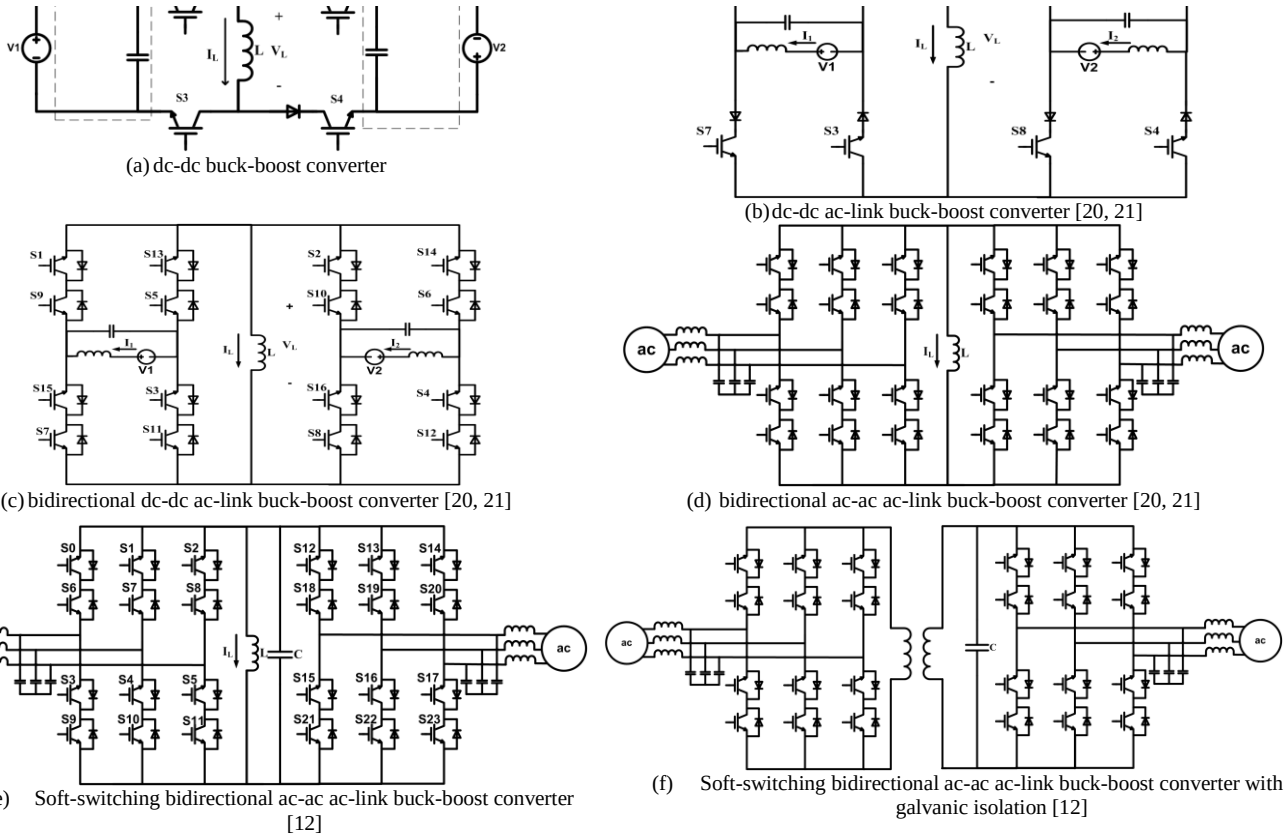

(a) dc-dc buck-boost converter

(b) dc-dc ac-link buck-boost converter [20, 21]

(c) bidirectional dc-dc ac-link buck-boost converter [20, 21]

(d) bidirectional ac-ac ac-link buck-boost converter [20, 21]

(e) Soft-switching bidirectional ac-ac ac-link buck-boost converter [12]

(f) Soft-switching bidirectional ac-ac ac-link buck-boost converter with galvanic isolation [12]

Fig. 1 The evolution of the soft switching ac-ac ac-link buck-boost converter [20, 21]

This article has been accepted for publication in a future issue of this journal, but has not been fully edited. Content may change prior to final publication. Citation information: DOI 10.1109/TIE.2014.2331011, IEEE Transactions on Industrial Electronics

converter is the capability of the converter to control the input power factor. This feature will be verified here. Moreover, the efficiency and the switch current rating of this converter and the dc-link converter are compared in this paper. These two converters have not been compared before.

II. Brief Overview on Principles of Operation

Fig. 1 represents the evolution of the soft-switching ac-link ac-ac buck-boost converter. The steps taken to form this converter from the basic dc-dc converter are illustrated in this figure. Fig. 1 (a) represents the simple dc-dc buck-boost converter. It is clear that switches S2, S3, S4, and the bottom diode are not necessarily needed. Assuming this converter operates at the boundary of the continuous and discontinuous conduction modes, by adding four other switches (switches S5-S8), as illustrated in Fig. 1 (b), the current of the link may become alternating. In this converter, during the first half cycle of the link, switches S1-S4 are involved and converter operates similar to the converter shown in Fig. 1 (a). During the second half cycle of the link, switches S5-S8 are involved and the link charges and discharges in a negative direction. Adding eight other switches makes it possible for the converter to have a bidirectional flow of power. This configuration is shown in Fig. 1 (c). By adding more legs to the input and output switch-bridges, the ac-link ac-ac buck-boost converter, represented in Fig. 1 (d), is formed. By adding a small capacitor to the link, the converter can provide soft-switching as well. The soft switching ac-link ac-ac buck-boost converter is shown in Fig. 1

shown in Fig. 1 (f). In practice, when the transformer is added, the link capacitor needs to be split into two capacitors placed at the primary and the secondary of the transformer. This is due to the leakage inductance of the transformer, the current of which cannot change instantaneously. Since the principles of the operation of the galvanically isolated and non-galvaically isolated converters are the same, in this paper, the main focus will be on the original configuration, which is shown in Fig. 1 (e).

Similar to the dc-dc buck-boost converter, this converter transfers power entirely through the link inductor. The link is charged through the input phase pairs and then discharged into the output phase pairs. Charging and discharging take place alternately. The frequency of charge/discharge is called the link frequency and is typically much higher than the input/output line frequencies. Between each charging and discharging, there is a resonating mode during which none of the switches conduct and the LC link resonates to facilitate the zero voltage turn-on and the soft turn-off of the switches. Due to the existence of the bidirectional switches, charging and discharging of the link in a reverse direction is feasible, leading to an alternating link current. The alternating link current results in better utilization of the inductor.

In an ac-ac converter, there are three input phases and one link to be charged through these input phases. In order to have more control on the currents, close to unity or desired Power Factor (PF) at the input, and minimized harmonics, the link charging mode is split into two modes. Although there are three phase-pairs in a three-phase system, considering the polarity of the current in each phase, only two of these phase-pairs can provide a path for the current when connected to the link. Similarly, the link discharge can be split into two modes. Again between each charging or discharging mode there is a resonating mode, which facilitates the zero voltage turn-on of the switches.

During the first half cycle of the link, the inductor is charged and discharged in the positive direction, and during the second half cycle of the link, it is charged and discharged in a negative direction. Each link cycle is divided into 16 modes, with 8 power transfer modes and 8 partial resonant modes taking place alternately. The link is energized from the input phase pairs during modes 1, 3, 9 and 11, and it is de-energized to the output phase pairs during modes 5, 7, 13 and 15. Before the start of mode 1 the incoming switches, the input switches which are supposed to conduct during modes 1 and 3, are turned on; however, they do not conduct immediately since they are reverse biased. Once the link voltage, which is resonating before mode 1, becomes equal to the maximum input line-to-line voltage, proper switches are forward biased initiating mode 1. The link charges until the current of one of the input-side phases averaged over a cycle time, meets its reference value. The conducting switch at that leg is then turned off. During mode 2 none of the switches conduct and the link resonates until its voltage becomes equal to that of the input phase pair having the second highest voltage. This is the phase pair the link charges next from. At this point, the proper switches are

turned off initiating another resonating mode. During mode 4, the behavior of the circuit is similar to that of mode 2 and the link voltage decreases until it reaches zero. At this point the output switches that are supposed to conduct during modes 5 and 7 are turned on; however being reverse biased they do not conduct. Once the link voltage, which is negative at this point, becomes equal to the output phase-pair which is supposed to be charged from the link, the proper switches will be forward biased and they start to conduct initiating mode 5. During mode 5 the link is discharged and once the current of one of the output phases averaged over the cycle meets its reference, the conducting switch on that leg is turned off. During mode 6 the link is allowed to swing to the voltage of the other output phase pair chosen during Mode 4. During mode 7, the link discharges to the selected output phase pair until there is just sufficient energy left in the link to swing to a predetermined voltage (V_{max}) which is slightly higher than the maximum input and output line to line voltages. At the end of mode 7 all the switches are turned off allowing the link to resonate during mode 8. Modes 9 through 16 are similar to modes 1 through 8, except that the link charges and discharges in the reverse direction. Fig. 2 depicts the link voltage, the link current and the unfiltered currents. Detailed study of different modes of operation can be found in [20].

In this converter, the switches which are supposed to be turned on during modes 4 and 8 are determined according to the current references. During mode 4, three switches at the output-

This article has been accepted for publication in a future issue of this journal, but has not been fully edited. Content may change prior to final publication. Citation information: DOI 10.1109/TIE.2014.2331011, IEEE Transactions on Industrial Electronics

side are turned on. The polarity of the output current references and also the link current determine the switches that need to be turned on. These switches should provide the desired polarity of the current at the output and also provide the proper polarity of the link current. At each cycle there are only three switches that satisfy the desired conditions. Assuming the positive direction in the output phases is from left to right and the positive link current is from top to bottom, for positive currents at the output phase "a" and link inductor and negative currents at output phases "b" and "c", switches S13, S14, and S15 need to be turned on. A similar method is used during mode 8 to turn on the proper switches at the input-side. The input-side current references indicate the power factor as well. Turning on the switches according to the current references, guaranties that the desired power factor would be provided.

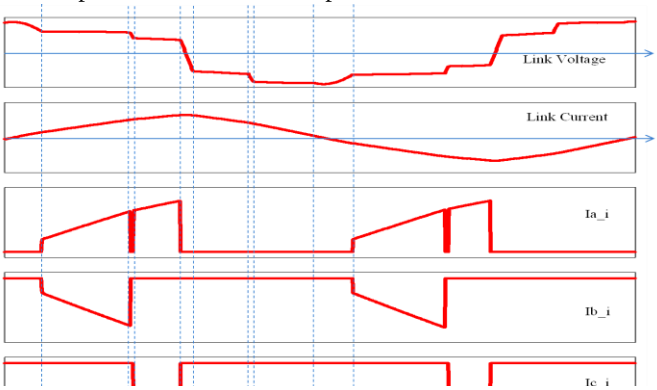

Fig. 2 Link voltage, link current and unfiltered currents during modes 1-16

The output current references are usually given or can be derived from the required load power. The input current references may be determined using the required load power and estimating the power losses.

In this converter, the average current control method is used. The switches corresponding to each input phase are turned off when the average of the unfiltered current in that phase meets the average of its reference, and once this happens the average of the current in that phase and also the average of the reference current corresponding to that phase will be both reset. Similarly, the output-side switches are turned off when the average of the unfiltered phase currents meet their references (mode 5) or when there is just enough energy left in the link to allow the link voltage to swing to V_{max} (mode 7). Fig. 3 shows the input side unfiltered currents, their references and the average of the phase currents and their references in one link cycle.

Fig. 4, Summarizes the control algorithm.

As mentioned earlier by using the estimated input power, the input current references are calculated and the link will be charged just as much as needed to meet the output current references. The other method (modified control method) is to charge the link more than it is needed by using a minimum efficiency value like 80% to estimate the input power. Similar to the original method, in this method the link will be charged from the input side during modes 1 and 3, and it will be discharged into the output phase pairs during modes 5 and 7. As mentioned earlier, in the original control method mode 5 is over when the current of one of the output phases meets its reference; whereas mode 7 is over when the link is almost discharged and there is just enough energy left in the link to swing to a predetermined voltage. In the modified control method, mode 7 will be also over when the current of another output phase meets its reference. This way, there will be some energy left in the link because the link has been charged more than what was needed. Therefore, after mode 7 the remaining energy needs to be discharged back into the input side during some additional modes (modes 9-12). The input phase pairs that were involved in charging the link will be involved in discharging it as well. Once the link is fully discharged, the second half cycle of the link starts by charging the link. By using this control method there is no need to estimate the input side currents, and the control is closed-loop.

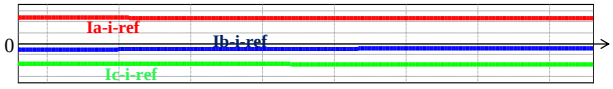

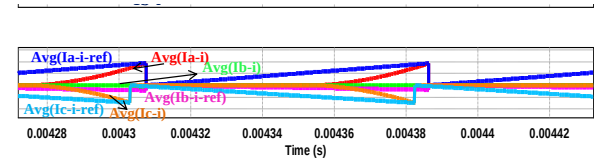

Fig. 3 Average current control in soft-switching ac-link ac-ac buck-boost converter: references of the unfiltered input currents, unfiltered input currents, and the average of the unfiltered currents and their references

III. Design and Analysis

To simplify the design procedure, the resonating time, which is much shorter than the power transfer time at full power, will be neglected. Moreover, charging and discharging are each assumed to take place in one equivalent mode, instead of two modes during each power cycle (each link cycle contains two power cycles). For this, the link is assumed to be charged through a virtual source with the input equivalent current and voltage. In a similar manner, the link is assumed to be discharged into a virtual load with the output equivalent current and voltage. Because the phase carrying the maximum input current is involved in the energizing of the link during both modes 1 and 3 and similarly, the phase carrying the maximum output current is involved in the de-energizing of the link during both modes 5 and 7, the input and output equivalent currents in this converter can be calculated as follows:

$$I_{i-eq} = \frac{3I_{i,peak}}{\pi} \quad (1)$$

$$I_{o-eq} = \frac{3I_{o,peak}}{\pi} \quad (2)$$

This article has been accepted for publication in a future issue of this journal, but has not been fully edited. Content may change prior to final publication. Citation information: DOI 10.1109/TIE.2014.2331011, IEEE Transactions on Industrial Electronics

Where $I_{i,peak}$ and $I_{o,peak}$ are the input and output peak phase currents. It can be shown that input and output equivalent voltages are equal to:

$$V_{i-eq} = \frac{\pi V_{i,peak}}{2}\cos\theta_i \qquad (3)$$

$$V_{o-eq} = \frac{\pi V_{o,peak}}{2}\cos\theta_o \qquad (4)$$

Where $V_{i,peak}$, $V_{o,peak}$, $cos(\theta_i)$, and $cos(\theta_o)$ are the input peak phase voltage, the output peak phase voltage, the input power factor, and the output power factor, respectively.

Fig. 5 represents one cycle of the link current as considered for the design. The following equations describe the behavior of the circuit during the charging and discharging of the link:

$$I_{Link,peak} = \frac{V_{i-eq}t_{charge}}{L} \qquad (5)$$

$$I_{Link,peak} = \frac{V_{o-eq}t_{discharge}}{L} \qquad (6)$$

In (5) and (6) $I_{Link,peak}$, t_{charge}, and $t_{discharge}$ represent the link peak current, the total charge time during modes 1 and 3, and the total discharge time during modes 5 and 7, respectively. Equations (5) and (6) determine the relationship between the charge time and discharge time as follows:

$$t_{charge} = \frac{V_{o-eq}t_{discharge}}{V_{i-eq}} \qquad (7)$$

It can be shown that the peak of filtered input and output currents determine the link peak current as follows [17]:

$$I_{Link,peak} = 2I_{i-eq}\left(1+\frac{V_{i-eq}}{V_{o-eq}}\right) = 2\left(I_{i-eq}+I_{o-eq}\right) \qquad (8)$$

The frequency of the link, f, can be chosen based on the power rating of the system and the characteristics of the

properly regulate the currents, at least two samples in each charging or discharging mode should be read. Once the link frequency is chosen, the following equation determines the inductance of the link:

$$L = \frac{P}{f\left(I^2_{Link,peak}\right)} \qquad (9)$$

where P is the rated power.

Link capacitance is chosen such that the resonating periods are retained within a small percentage of the link cycle. Since no power is transferred during the resonating time, the resonating modes must be kept as short as possible:

$$\frac{1}{2\pi\sqrt{LC}} \gg f \qquad (10)$$

As mentioned earlier, the resonating time is normally negligible at full power. At lower power levels, the power transfer time (energizing and de-energizing time) is usually shorter than the power transfer time at full power, whereas the resonating time is almost constant. Therefore, the resonating time cannot be neglected at low power levels. Fig. 6 shows the link voltage and current over one cycle, assuming the resonating time is not negligible.

If the resonating time is negligible, (8) and (9) may be used to calculate the link peak current and the link frequency at different power levels. However, when the resonating time cannot be neglected the analysis will be more complicated.

Considering the principles of operation, the link current at the end of the de-energizing mode (I_4 in Fig. 6) can be calculated by:

$$I_4 = \sqrt{\frac{C}{L}\left(V^2_{max} - V^2_{o,eq}\right)} \qquad (11)$$

V_{max}, as explained in the principles of operation, is an optional value slightly higher than the maximum input and output line-to-line voltages, whichever is higher. This value should not be much higher than the peak of the input and output line-to-line voltages, because the higher V_{max} is, the longer the resonating time during mode 8 will be. Since no power is transferred during this mode, it needs to be kept as short as possible. A reasonable value for V_{max} may be 15% more than the maximum peak of the input or output line-to-line voltage (whichever is higher).

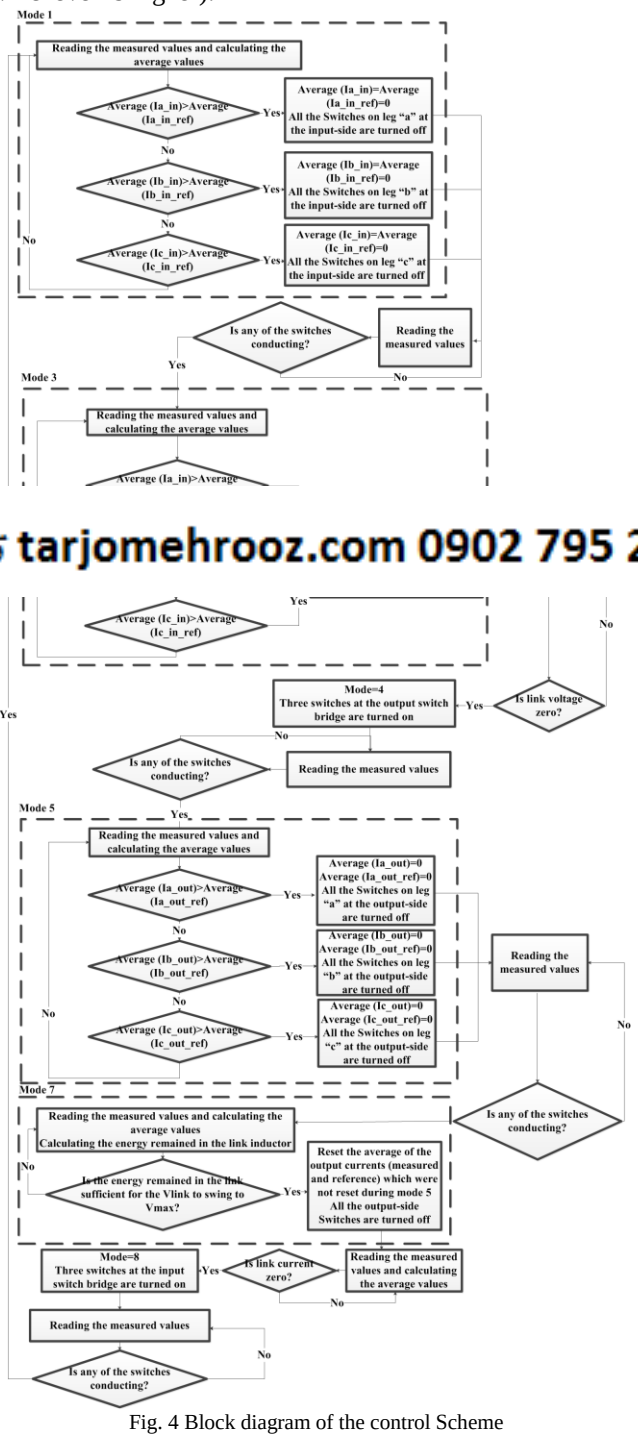

Fig. 4 Block diagram of the control Scheme

This article has been accepted for publication in a future issue of this journal, but has not been fully edited. Content may change prior to final publication. Citation information: DOI 10.1109/TIE.2014.2331011, IEEE Transactions on Industrial Electronics

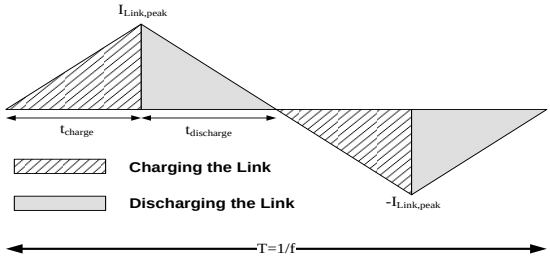

Fig. 5 One cycle of the link current as simplified for the design procedure

Solving the resonant LC circuit during the time period t_1 (resonating mode that occurs after the de-energizing and before the energizing modes), I_1 (link current at the beginning of the energizing mode) and t_1 can be calculated as follows:

$$I_1 = \sqrt{\left(I_4^2 + \left(\frac{V_{o,eq}}{L\omega_r}\right)^2 - \left(\frac{V_{i,eq}}{L\omega_r}\right)^2\right)} \qquad (12)$$

$$t_1 = \frac{1}{\omega_r}\left(\pi + \text{TAN}^{-1}\left(\frac{I_1 L\omega_r}{V_{i,eq}}\right) - \pi + \text{TAN}^{-1}\left(\frac{I_4 L\omega_r}{V_{o,eq}}\right)\right) = \frac{1}{\omega_r}\left(\text{TAN}^{-1}\left(\frac{I_1 L\omega_r}{V_{i,eq}}\right) + \text{TAN}^{-1}\left(\frac{I_4 L\omega_r}{V_{o,eq}}\right)\right) \qquad (13)$$

In the above equations, ω_r is the resonance angular frequency that can be calculated by:

$$\omega_r = \frac{1}{\sqrt{LC}} \qquad (14)$$

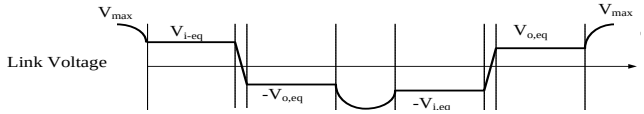

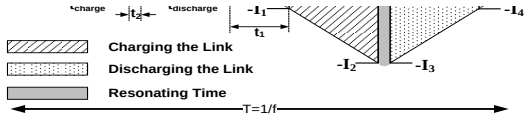

Fig. 6 The link voltage and current over one cycle when the resonating time is not negligible

In order to find the link peak current and the link frequency, first the current at the end of the energizing mode (I_2), the current at the beginning of the de-energizing mode (I_3), the resonating time after the energizing mode and before the de-energizing mode (t_2), and the total energizing and de-energizing time should be determined. Five other equations should be solved to determine I_2, I_3, t_2, t_{charge}, and $t_{discharge}$. These equations are as follows:

$$V_{i,eq} = L\frac{I_2 - I_1}{t_{charge}} \qquad (15)$$

$$V_{o,eq} = L\frac{I_3 - I_4}{t_{discharge}} \qquad (16)$$

$$I_{i,eq} = \frac{t_{charge}}{2(t_{charge}+t_{discharge}+t_1+t_2)}(I_2+I_1) \qquad (17)$$

$$I_{o,eq} = \frac{t_{discharge}}{2(t_{charge}+t_{discharge}+t_1+t_2)}(I_3+I_4) \qquad (18)$$

$$t_2 = \frac{1}{\omega_r}\left(\pi - \text{TAN}^{-1}\left(\frac{I_3 L\omega_r}{V_{o,eq}}\right) - \text{TAN}^{-1}\left(\frac{I_2 L\omega_r}{V_{i,eq}}\right)\right) \qquad (19)$$

Once these equations are solved, $I_{Link,peak}$ and f can be calculated as follows:

$$I_{Link,peak} = \sqrt{\left(I_2^2 + \left(\frac{V_{i,eq}}{L\omega_r}\right)^2\right)} \qquad (20)$$

$$f = \frac{1}{2(t_{charge}+t_{discharge}+t_1+t_2)} \qquad (21)$$

It can be shown that by decreasing the power level, the link peak current decreases, whereas the link frequency increases. The maximum link frequency, which occurs at zero power, is equal to the resonant frequency, which is equal to $\frac{1}{2\pi\sqrt{LC}}$. Fig. 7 represents the link peak current and the link frequency variations vs. power.

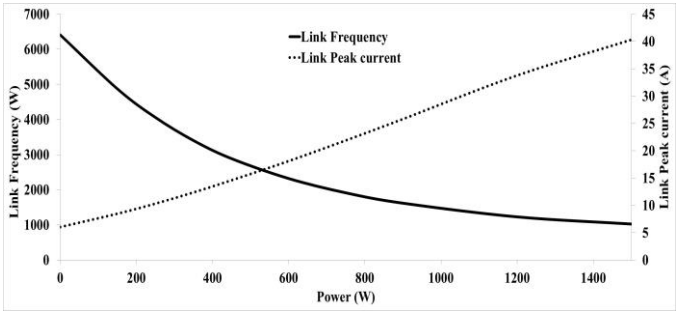

Fig. 7 Link peak current and link frequency variations vs. power in the designed 1.5 kW ac-link converter

IV. COMPARISON OF THE SOFT-SWITCHING AC-LINK AC-AC BUCK-BOOST AND THE CONVENTIONAL DC-LINK CONVERTERS

As mentioned earlier, the proposed converter is an excellent alternative to conventional dc-link converters. In this section

current of the input and output switches are as follows:

$$I_{SW-Input} = \frac{1}{2\pi} I_{i,peak} \qquad (22)$$

$$I_{SW-Output} = \frac{1}{2\pi} I_{o,peak} \qquad (23)$$

Therefore, the average current of the switches in this converter are half the average current of the switches in the dc-link converter.

Another important criterion based on which these converters may be compared, is the efficiency. The main sources of power dissipation in the soft-switching ac-link ac-ac buck-boost converter are the conduction loss of the switches, the link inductor copper loss, and the link inductor core loss. Switches S0–S5 at the input side and S12–S17 at the output side may conduct only during the half cycles that that the link current is positive. Switches S6–S11 and S18–S23 may conduct during the half cycles that the link current is negative. Therefore, the conduction loss of each switch at the input side and at the output side may be estimated as follows:

$$(0\le m\le 11)\quad P_{Sm} = \frac{1}{T}\int_0^T \left(V_{CE(sat)} i_S(t)dt\right) = V_{TO,S} I_{Si,avg} + r_{T,S} I_{Si,rms}^2 = \frac{1}{2\pi} I_{i,peak} V_{TO,S} + \frac{1}{4} r_{T,S} I_{in,unfiltered,rms}^2 \qquad (24)$$

$$(12\le m\le 23)\quad P_{Sm} = \frac{1}{T}\int_0^T \left(V_{CE(sat)} i_S(t)dt\right) = V_{TO,S} I_{So,avg} + r_{T,S} I_{So,rms}^2 = \frac{1}{2\pi} I_{o,peak} V_{TO,S} + \frac{1}{4} r_{T,S} I_{out,unfiltered,rms}^2 \qquad (25)$$

In the above equations, $i_S(t)$, $V_{CE(sat)}$, $V_{TO,S}$, $r_{T,S}$, $I_{Si,rms}$, $I_{So,rms}$, $I_{Si,avg}$, $I_{So,avg}$, , $I_{in,unfiltered,rms}$, $I_{out,unfiltered,rms}$, are the IGBT instantaneous current, IGBT collector emitter saturation voltage, IGBT threshold voltage, IGBT series resistance, the

This article has been accepted for publication in a future issue of this journal, but has not been fully edited. Content may change prior to final publication. Citation information: DOI 10.1109/TIE.2014.2331011, IEEE Transactions on Industrial Electronics

input-side switch rms current, output-side switch rms current, the input-side switch average current, the output-side switch average current, the rms of the input-side unfiltered current, and the rms of the output-side unfiltered current, respectively. Given that the current passing each IGBT is equal to the current passing the anti-parallel diode of the IGBT placed in series with that IGBT, the total conduction loss in this converter is equal to:

$$P_{Conduction} = \frac{6}{\pi}\left(I_{i,peak} + I_{o,peak}\right)\left(V_{TO,S} + V_{TO,D}\right) + 3\left(I^2_{in,unfiltered,rms} + I^2_{out,unfiltered,rms}\right)\left(r_{T,S} + r_{T,D}\right) \quad (26)$$

Where, $V_{TO,D}$ and $r_{T,D}$ are the diode threshold voltage and series resistance, respectively.

When using reverse blocking IGBTs, the conduction losses may become almost half, as the bidirectional switches may be formed by placing two IGBTs in parallel instead of series. In this case the conduction losses may be estimated by the following equation:

$$P_{Conduction\_RB} = \frac{6}{\pi}\left(I_{i,peak} + I_{o,peak}\right)\left(V_{TO,S}\right) + 3\left(I^2_{in,unfiltered,rms} + I^2_{out,unfiltered,rms}\right)\left(r_{T,S}\right) \quad (27)$$

A 1.5 kW soft-switching ac-link ac-ac buck-boost converter was designed, and its parameters are listed in Table 1. The link capacitance can be much smaller, e.g. 100 nF; however, due to the limitations that we had for experimental evaluation of the converter, a 400 nF link capacitor was chosen. In the prototype a microcontroller is used for implementing the control algorithm, considering the noticeable calculation time, and to

Molypermalloy Powder (MPP) cores were used for the link inductor. For the selected cores, the copper loss and the core loss are calculated as follows [22]:

$$P_{Copper} = 0.0376 * I^2_{Link,Peak} \quad (28)$$

$$P_{Core} = 8.57 * 10^{-6} * f^{1.65} \quad (29)$$

The copper loss increases by increasing the power level; whereas the core loss decreases by increasing the power level.

Fig. 8 shows the efficiency of the designed converter over a range of power. In this figure, the efficiency of a 1.5 kW dc-link converter with the same input and output specifications as the ac-link converter is shown as well. The link voltage in the dc-link converter is 470 V. Depending on the switching frequency and the characteristics of the switches in the dc-link converter, the efficiency of this converter may be higher or lower than the proposed converter. In Fig. 8 the efficiency of the dc-link converter with 4 kHz and 8 kHz switching frequencies are shown. The efficiency of the dc-link converter with 4 kHz switching frequency is higher than that of the proposed converter. However, by increasing the switching frequency to 8 kHz, the efficiency of the dc-link converter will become lower.

V. Simulation and Experimental Results

In this part the performance of the soft-switching ac-link ac-ac buck-boost converter will be evaluated through simulations and experiments. A low power converter with the parameters listed in Table 1 is designed.

This converter was simulated in PSim and Figs. 9-13 represent the results. Fig. 9 shows the input current and voltage when the converter operates at 450 W. As seen in this figure the input current and voltage are about 25 degrees apart. As mentioned earlier one of the advantages of this converter and the proposed control algorithm is the possibility of controlling the input power factor. In this simulation we have controlled the unfiltered current such that it is in phase with the phase voltage. However, the input filter capacitor, which is 40 µF, causes the filtered current to be phase shifted from the unfiltered current. To show that the input power factor can be controlled, in Fig. 10 the simulation is repeated but this time the input current is regulated such that the filtered current is in phase with the voltage.

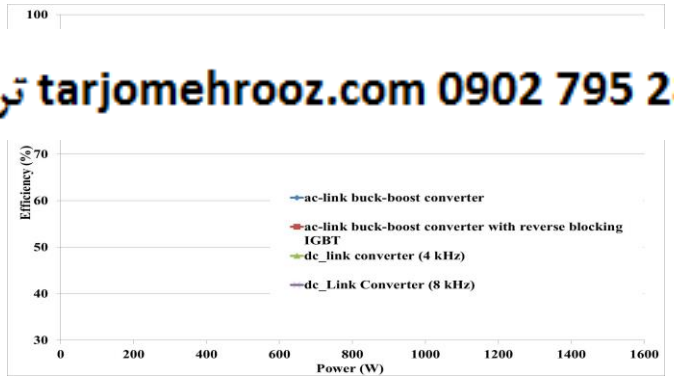

Fig. 8 Efficiency of the dc-link and soft-switching ac-link converters

It should be noted that the filtered currents are referred to the sinusoidal currents passing the filter inductors, whereas the unfiltered currents are the discontinuous currents at the terminals of the converter as shown in Fig.2. Fig. 11 represents the output voltage and current. Since the load is resistive the output power factor is unity, too. Fig. 12 depicts the link current

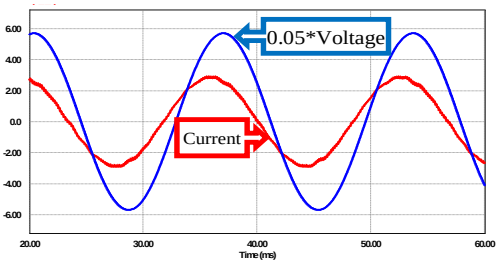

Fig. 9 The input-side current and scaled voltage when the current is regulated such that the unfiltered current is in-phase with the input voltage (filtered current and voltage have phase shift)

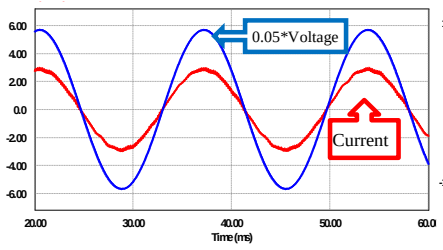

Fig. 10 The input-side current and scaled voltage when the current is regulated such that the filtered current is in-phase with the input voltage

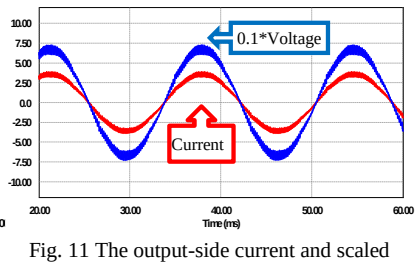

Fig. 11 The output-side current and scaled voltage

This article has been accepted for publication in a future issue of this journal, but has not been fully edited. Content may change prior to final publication. Citation information: DOI 10.1109/TIE.2014.2331011, IEEE Transactions on Industrial Electronics

and voltage. The link peak current varies between 14 A and 14.7 A. Therefore, the average of the link peak current is about 14.3 A. This value is much higher than the value calculated by (8). This is due to the high link capacitance. A lower link capacitance is always more desirable in this converter. Since no power is transferred during the resonance, the resonating time should be kept as short as possible. However, in practice we have to make sure that the proper switches are turned on before they are forward biased; otherwise the switches will have hard switching. Therefore, the sampling time of the microcontroller should be shorter than the length of mode 4, which is approximately equal to t_2, and may be calculated from (19). By optimizing the control code and using a faster microcontroller, the sampling time of the microcontroller may be decreased and a lower link capacitance can be chosen. Fig. 13 shows the link current and voltage when the link capacitance is decreased to 20 µF. The link current in this case has dropped to 11.55 A. This value is very close to the value calculated by (8), which is 11.74 A.

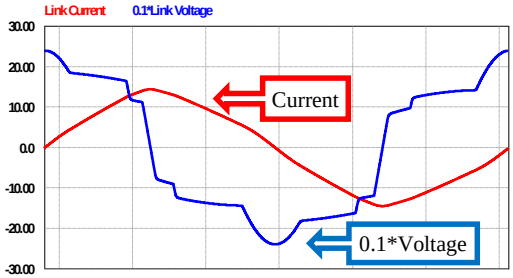

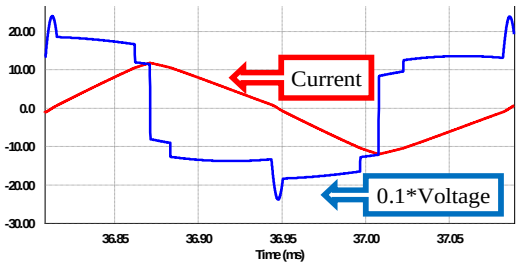

Fig. 13 the link current and scaled link voltage when using 20 µF link capacitance

A low power prototype with the same specifications as listed in table 1 has been fabricated. Fig. 14 represents the input current and voltage when the converter is operating at 450 W. As seen in this figure the input current and voltage are not in phase. Again the converter is controlled such that the unfiltered current is in phase with the voltage. Considering that the frequency of the unfiltered phase currents is twice the frequency of the link, the cut-off frequency of the filters can be very high and the filter inductance and capacitance can be small in this converter. The first limitation of the filter inductance (L_f) and filter capacitance (C_f) is as follows:

$$\frac{1}{2\pi\sqrt{L_f C_f}} < 2f \qquad (30)$$

The filter capacitance may be chosen such that the rms of the current passing through the filter capacitor is just a small percentage of the rms of the phase current. Once the filter capacitance is determined, the filter inductance may be chosen using (30). The filter components are expected to be small in this converter, because the link frequency is high.

However, the three-phase ac voltage source used in this test was highly distorted by low frequency harmonics, including the 5th harmonic. In order to attenuate the low frequency harmonics of the current, which are generated by the same order harmonics of the voltage, a high inductance filter was chosen at the input (15 mH). The input current with 1 mH input filter inductance is shown in Fig. 15. As seen in this figure, the current contains the low frequency harmonics.

Fig. 16 represents the load current and voltage. Similar to the simulations, a three-phase resistive load is used. In this test both the input and output frequencies are 60 Hz. To show the capability of the converter in changing the frequency, the test was repeated and the output frequency was set at 30 Hz while the frequency of the input voltage/current was still 60 Hz. Fig. 17 shows the output current/voltage corresponding to this case.

The link current and voltage are depicted in Fig. 18. The link peak current and the link frequency are 14.2 A and 3.1 kHz, respectively. These values are very close to the values achieved through the simulation. Using the method introduced in section III for calculating the accurate values of the link peak current and the link frequency, these parameters are determined as 14.3 A and 3.1 kHz, respectively. This verifies the accuracy of the method proposed in section III. In this test the sampling frequency is 200 kHz.

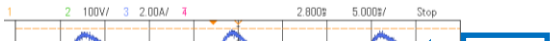

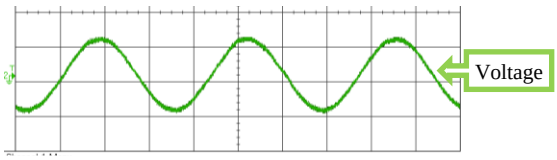

Fig. 14 input current (2 A/div) and voltage (100 V/div) in step-down operation and with 15 mH input filter inductance (experiment), time scale: 5 ms/div

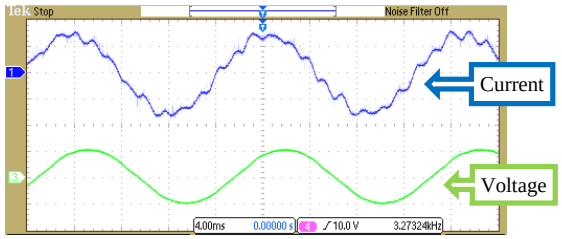

Fig. 15 Input current (2 A/div) and voltage (100 V/div) in step-down operation and with 1 mH input filter inductance (experiment), time scale: 4 ms/div

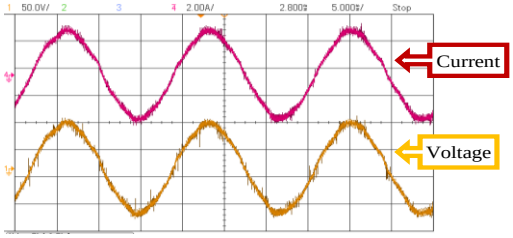

Fig. 16 The load current (2 A/div) and voltage (50 V/div) in step-down operation (experiment, time scale: 5 ms/div

This article has been accepted for publication in a future issue of this journal, but has not been fully edited. Content may change prior to final publication. Citation information: DOI 10.1109/TIE.2014.2331011, IEEE Transactions on Industrial Electronics

To verify the experimental results, the simulation was repeated by including the low-frequency harmonics in the input voltage source model. Fig. 19 shows the input-side current when 1 mH inductors are used at the input. The link current/voltage and the load current are not affected, because in this converter only the unfiltered currents are measured and used by the controller. The input current in the same system with a 15 mH input filter inductance is depicted in Fig. 20.

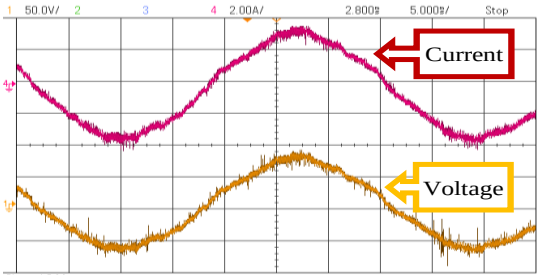

Fig. 17 Load current (2 A/div) and voltage (50 V/div) when the frequency is set at 30 Hz (experimental results), time scale: 5 ms/div

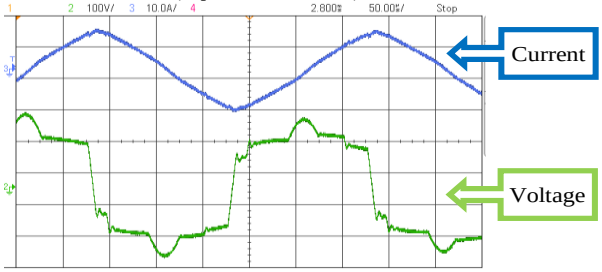

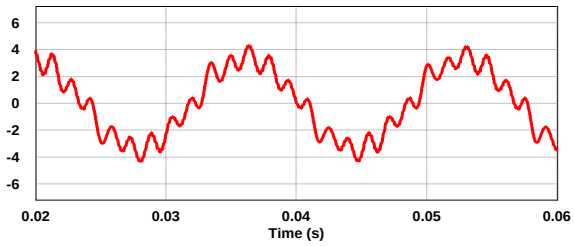

Fig. 19 The input-side current when the input voltage is polluted by low-frequency harmonics and 1 mH filter inductance is used (Simulation)

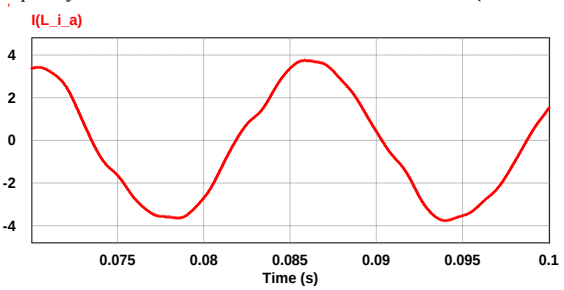

Fig. 20 The input-side current when the input voltage is polluted by low-frequency harmonics and 15 mH filter inductance is used (Simulation)

In Figs. 14-20 the peak of the input voltage is higher than the peak of the output voltage. Therefore, the converter is stepping down the voltage. Figs. 21-23 illustrate the experimental results corresponding to the step-up operation of the converter with 70 V input and 120 V output voltages. The input current/ voltage, the output current/voltage, and the link current/voltage corresponding to this case are shown in these figures.

To validate the method proposed in section III, the measured link peak current and frequency at two different power levels are compared with the values achieved through the simulation and analysis. These values are compared in Table 2. As seen in this table, the proposed method is accurate and its error is less than 3%.

Fig. 24 verifies the zero voltage turn-on of the switches. This figure depicts the current passing an output-side bidirectional switch (S12+S18) and the voltage across this bidirectional switch. The switch voltage here shows $-V_{CE}$ of the conducting switch; therefore, when this voltage is positive the conducting switch is reverse biased. As seen in this figure, this switch does not conduct before its voltage reaches zero.

The measured efficiency and the calculated efficiency of the converter with the parameters listed in Table 1, is depicted in Fig. 25.

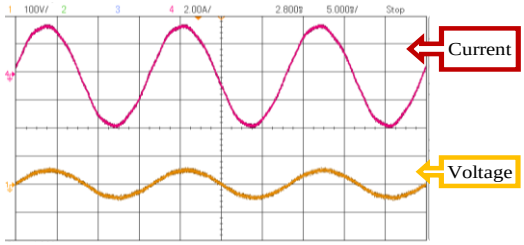

Fig. 21 The input current (2 A/div) and voltage (100 V/div) in boost operation (Experiment), time scale: 5 ms/div

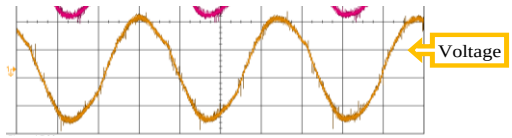

Fig. 22 The load current (1 A/div) and voltage (50 V/div) in boost operation (Experiment), time scale: 5 ms/div

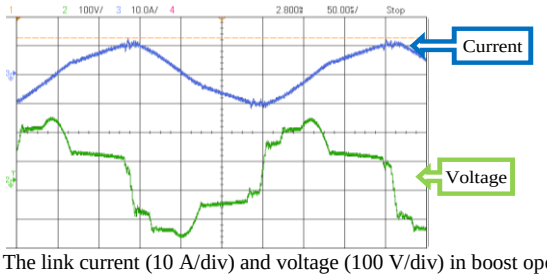

Fig. 23 The link current (10 A/div) and voltage (100 V/div) in boost operation (Experiment), time scale: 50 µs/div

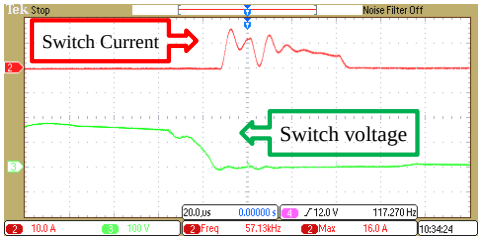

Fig. 24 Current passing switches S12 and S18 (10 A/div), voltage across S12+S18 (100 V/div), and the link current (10 A/div), time scale: 20 µs/div

This article has been accepted for publication in a future issue of this journal, but has not been fully edited. Content may change prior to final publication. Citation information: DOI 10.1109/TIE.2014.2331011, IEEE Transactions on Industrial Electronics

TABLE 1 PARAMETERS OF THE CONVERTERS

Parameter	Value/ Part number
Input Voltage	140 V
Output Voltage	92 V
Input side filter inductance	1 mH and 15 mH
Input side filter capacitance	40 µF
Output side filter inductance	556 µH
Output side filter capacitance	20 µF
IGBT	IRG7PH42UDPBF-ND: V_{CES}=1200 V, I_C=45 A
AC-Link Converter	
Link inductance	880 µH
Link Capacitance	700 nF
DC-Link Converter	
Link Capacitance	200 µF

This new class of power converters does not have any limitations on the load type. A 30 kW soft-switching ac-link dc-ac buck-boost inverter with the specifications listed in [19], was used to drive a 20 hp induction motor operating at no load condition. Fig. 26 shows the stator current and line to line voltage when the speed of the machine is low. The load frequency is 8 Hz in this case.

The experimental results of the same inverter connected to the grid were published in [19]. Fig. 27 shows the load current and line-to-neutral voltage when the inverter is running at 25 kW. As discussed in [19], the load current contains some low frequency harmonics the source of which is the low frequency components of the grid voltage. Due to the existence of

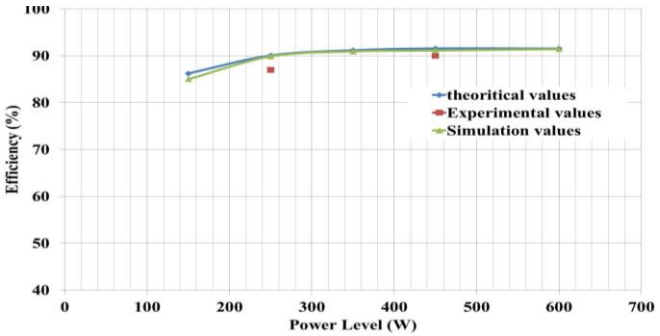

Fig. 25 Efficiency of the proposed converter

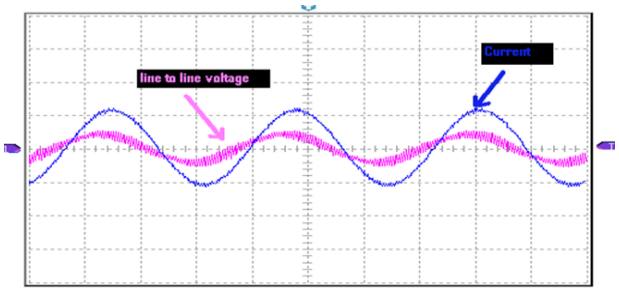

Fig. 26 Stator current and line-to-line voltage when the soft-switching ac-link dc-ac buck-boost inverter drives an induction motor (voltage: 200V/div scale, current: 10A/div, time: 5 ms/div)

TABLE 2 SUMMARY OF ANALYSIS, SIMULATION AND EXPERIMENTAL RESULTS

Case	Parameter	Analysis	Simulation	Experiment
P_{in}=450W, V_{in}=140, V_o=92	I_{Link}	14.3 A	14.3 A	14.2 A
	F_{Link}	3.1 kHz	3.1 kHz	3.1 kHz
P_{in}=250 W, V_{in}= 140, V_o=92	I_{Link}	10.3 A	10.2 A	10.7 A
	F_{Link}	4.4 kHz	4.5 kHz	4.4 kHz

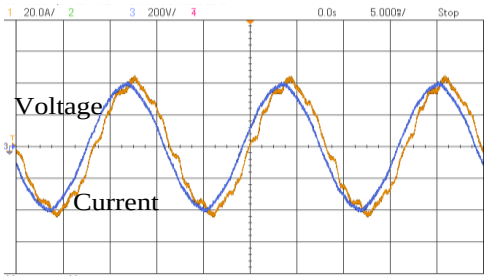

Fig. 27 Load current (20 A/ division) and line-to-neutral voltage (200 V/division) of the grid-tied soft-switching ac-link dc-ac buck-boost inverter running at 25 kW, time scale: 5 ms/div

VI. CONCLUSION

This paper presented detailed design and analysis of the soft-switching ac-link ac-ac buck-boost converter. The performance of the converter at low power levels, when the resonance of the link is not negligible, was studied and a method was proposed for calculating the link peak current and the link frequency at these power levels. It was shown that the link peak current

conventional dc-link converters. In this paper the current rating of the switches and the efficiency of the two converters were compared. The proposed converter requires more switches, but the average current of each switch in this converter is half the average current of the switches in the dc-link converter. Depending on the switching characteristics and the switching frequency in the dc-link converter, the efficiency of this converter may be higher or lower than that of the proposed converter. Clearly, if reverse blocking IGBTs are used the efficiency of the proposed converter increases significantly.

To control this converter, the input-side current references need to be estimated. However, by using a modified control scheme the need to know the input-side current references is eliminated and the converter may be controlled by knowing the output-side current references. The main limitation of this converter is its complicated control scheme that increases the calculation time of the microcontroller and limits the link frequency. By using an FPGA or simplifying the control scheme higher link frequencies may be achieved.

In this paper, the performance of the soft-switching ac-link ac-ac buck-boost converter was evaluated through both simulation and experimental results.

REFERENCES

[1] J. Rodriguez, S. Bernet, W. Bin, J.O. Pontt, S. Kouro, "Multilevel Voltage-Source-Converter Topologies for Industrial Medium-Voltage Drives," *IEEE Trans. Ind. Electron.*, vol. 54, no. 6, pp.2930-2945, 2007

[2] W. Bin, J.O. Pontt, J. Rodriguez, S. Bernet, S. Kouro, "Current-Source Converter and Cycloconverter Topologies for Industrial Medium-Voltage Drives," *IEEE Trans. Ind. Electron.*, vol. 55, no. 7, pp.2786-2797, 2008

[3] F.L. Luo , Y. Hong, "Power Electronics: Advanced Conversion Technologies", CRC Press, 2010

[4] J. W. Kolar, T. Friedli, J. Rodriguez, P. W. Wheeler, "Review of Three-Phase PWM AC–AC Converter Topologies," *IEEE Trans. Ind. Electron.*, vol.58, no.11, pp.4988-5006, 2011

[5] S. Chakraborty, B. Kramer, and B. Kroposki, "A review of power electronics interfaces for distributed energy systems towards achieving low-cost modular design," Renewable and Sustainable Energy Reviews, vol. 13, pp. 2323-2335, 2009

[6] G. Grandi, C. Rossi, D. Ostojic, and D. Casadei, "A New Multilevel Conversion Structure for Grid-Connected PV Applications," *IEEE Trans. Ind. Electron.*, vol. 56, pp. 4416-4426, 2009

[7] T. Kerekes, R. Teodorescu, P. Rodriguez, G. Vazquez, and E. Aldabas, "A New High-Efficiency Single-Phase Transformerless PV Inverter Topology," *IEEE Trans. Ind. Electron.*, vol. 58, pp. 184-191, 2011

[8] T.A. Lipo, "Reson ant link converters: a new direction in solid state power conversion", presented at Second Int. Conf. Electrical Drives, Eforie Nord, Romania, Sept. 1988

[9] P.K. Sood, T.A. Lipo, and I.G. Hansen, "A versatile power converter for high frequency link systems", *IEEE Trans. Power Electron.*, vol. 3, no. 4, pp. 383-390, Oct 1988.

[10] K. Ngo, "Topology and Analysis in PWM Inversion, Rectification, and Cycloconversion", Ph.D. Dissertation, California Institute of Technology, 1984

[11] I.-D. Kim and G.-H. Cho, "New bilateral zero voltage switching ac/ac converter using high frequency partial-resonant link," *Proc. IEEE Industrial Electronics Society Annual Conference (IECON)*, 1990, pp. 857-862

[12] W.C. Alexander, "Universal Power Converter", US patent 2008/0013351A1, Jan.17, 2008

[13] A. Balakrishnan, H. A. Toliyat and W.C. Alexander, "Soft switched ac

[15] A. Balakrishnan, M. Amirabadi, H. Toliyat, W. Alexander, "Soft switched ac-link wind power converter", *Proc. IEEE International Conference on Sustainable Energy Technologies (ICSET)*, 2008, pp. 318-321

[16] M. Amirabadi, H.A. Toliyat and W. Alexander, "Battery-Utility Interface using Soft Switched AC Link supporting Low Voltage Ride Through", *Proc. IEEE Energy Conversion Congress and Exposition Conference (ECCE)*, 2009, pp. 2606-2613

[17] Amirabadi, H. A. Toliyat, and W. C. Alexander, "Partial resonant AC link converter: A highly reliable variable frequency drive," *Proc. Annual Conference on IEEE Industrial Electronics Society (IECON)*, 2012, pp. 1946-1951

[18] M. Amirabadi, H. Toliyat, W. Alexander, "A Multi-port ac Link PV Inverter with Reduced Size and Weight for stand-alone application", *IEEE Trans. Ind. Appl.*, vol.49, pp.2217-2228, 2013

[19] M. Amirabadi, A. Balakrishnan, H. Toliyat, W. Alexander, "High Frequency ac-Link PV Inverter", *IEEE Trans. Ind. Electron.*, vol. 61, pp. 281-291, 2014

[20] Mahshid Amirabadi, "Soft-Switching High-Frequency ac-Link Universal Power Converters with Galvanic Isolation," Ph.D. Dissertation, Texas A&M University, College Station, TX, 2013

[21] Mahshid Amirabadi, Hamid A. Toliyat, "AC-Link Universal Power Converters: A New Class of Power Converters for Renewable Energy and Transportation" in Power Electronics for Renewable Energy Systems, Transportation and Industrial Application, 1st ed., Haitham Abu-Rub, Mariusz Malinowski, Kamal Al-Haddad, Ed. New York, John Wiley & Sons, August 2014, pp. 107-135

[22] 2013 Magnetics Powder Core Catalog (2013, Oct. 3). Available: http://www.mag-inc.com/products/powder-cores/learn-more-about-powder-cores

Mahshid Amirabadi (S'05, M'13) received the B.S. degree from Shahid Beheshti University, Tehran, Iran in 2002, the M.S. degree from University of Tehran, Iran in 2006, and the Ph.D. degree from Texas A&M University in 2013, all in electrical engineering. She is currently an assistant professor at the University of Illinois at Chicago. Her main research interests and experience include design, analysis and control of power converters, renewable energy systems and variable speed drives.

Jeihoon Baek (S'03, M'10) received the B.S. and M.S. degrees in Electrical Engineering from Hongik University, Korea 1996 and 1998, respectively. He also obtained an M.S. degree in Electrical Engineering from University of Wisconsin-Madison in 2006, the Ph.D. degree in electrical engineering from Texas A&M University in 2009. From 1998 to 2000, he was with Amotech, Seoul, Korea. He was also with Samsung Electromechanics, Suwon, Korea as a senior research engineer from 2000 to 2003. From 2010 to 2013, he worked as a principal engineer at Samsung Advanced Institute of Technology, Youngin, Korea. Since 2014 he has been with Korea Railroad Research Institute, Uiwang, Korea. His current research interests and experiences are the design and analysis of electrical machies, variable speed drives for traction and propulsion applications and novel power conversion topology.

Hamid A. Toliyat (S'87, M'91, SM'96, F'08) is currently Raytheon endowed professor of electrical engineering. Dr. Toliyat has received the prestigious Cyrill Veinott Award from the IEEE Power Engineering Society in 2004 and has received numerous awards from Texas A&M University. He is the recipient of the 2008 Industrial Electronics Society Prize Paper Award. Prof. Toliyat has supervised more than 60 graduate students, post docs and research engineers, published over 420 technical papers, and has 15 issued and pending US patents. He is the co-author of DSP-Based Electromechanical Motion Control, CRC Press, 2003, the co-editor of Handbook of Electric Motors - 2nd Edition, Marcel Dekker, 2004, and the co-author of Electric Machines – Modeling, Condition Monitoring, and Fault Diagnosis, CRC Press, Florida, 2013.

William C. Alexander (M'95) received the Bachelor's and Master's degrees in engineering from the University of Texas, Austin, in 1976 and 1979, respectively.

He is the CTO and founder of Ideal Power Converters, Inc., Austin, a company formed to develop the soft-switched ac link power converter for motor drive, wind power, and solar inverter applications.

Mr. Alexander is a prolific inventor with over 15 granted US patents. He has over 25 years of experience in engineering including mechanical, electrical, electronic, and embedded software and HDL engineering, and is a registered Professional Engineer in State of Texas.